Environ Sci Pollut Res (2014) 21:13850–13866
DOI 10.1007/s11356-014-2895-7

Transcriptional responses and embryotoxic effects induced by pyrene and methylpyrene in Japanese medaka (*Oryzias latipes*) early life stages exposed to spiked sediments

Iris Barjhoux · Jérôme Cachot · Patrice Gonzalez · Hélène Budzinski · Karyn Le Menach · Laure Landi · Bénédicte Morin · Magalie Baudrimont

Received: 30 October 2013 / Accepted: 6 April 2014 / Published online: 23 April 2014

Abstract Japanese medaka (*Oryzias latipes*) embryos were exposed to sediments spiked with environmental concentrations (300 and 3,000 ng/g dry weight) of pyrene (Pyr) and methylpyrene (MePyr) throughout their development. Embryotoxicity, teratogenicity, and transcriptional responses (qRT-PCR) were analyzed in embryos and newly hatched larvae. The genotoxicity of the two polycyclic aromatic hydrocarbons (PAHs) was also tested in prolarvae using the comet assay. Exposure to each compound had a clear impact on embryonic development and resulted in several teratogenic effects, including cardiovascular injuries, reduced absorption of yolk sac reserves, and jaw and spinal deformities. Interestingly, the overall toxic effects of Pyr and MePyr considerably overlapped those induced following dioxin exposure. qRT-PCR analysis revealed the transcriptional induction of genes involved in mitochondrial energetic metabolism (*coxI*), xenobiotic biotransformation (*cyp1a*), and cell cycle regulation (*wnt1*) by the two PAHs. MePyr also activated cell cycle arrest (*p53*), oxidative DNA damage repair (*ogg1*), and retinoid-mediated (*raldh2* and *rarα1*) gene transcription. DNA damage was not found to be significantly increased following Pyr and MePyr exposure. The lack of significant genotoxic effect in comparison to the control might be the consequence of the efficient onset of DNA damage repair mechanisms as suggested by *ogg1* gene transcription upregulation. Results reported in the present study have brought new insights into the modes of action of Pyr, and the effects of MePyr exposure have been investigated in fish ELS for the first time.

Keywords PAH-spiked sediments · Fish early life stage · Gene expression · Embryotoxicity · Teratogenicity · Genotoxicity

Introduction

Polycyclic aromatic hydrocarbons (PAHs) are ubiquitous contaminants that are primarily introduced into the environment through anthropogenic activities such as the incomplete combustion of organic matter, fossil fuels, oil, and wood. Firstly released in the aquatic environment through land-based runoff, industrial and urban effluents, and atmospheric deposition, they get trapped in sediments due to their hydrophobic properties (Dupree and Ahrens 2007; Ineris 2006). Since many fish species use sediments as spawning substrate, PAHs can represent a long-term threat for aquatic ecosystems due to their persistence and their ability to pass through biological membranes and to accumulate in organisms.

For the past few decades, many studies have demonstrated the high sensitivity of fish early life stages (ELS) to PAH exposure (e.g., Li et al. 2011; Cachot et al. 2007; Farwell et al. 2006; Rhodes et al. 2005; Incardona et al. 2004; Carls et al. 1999). A wide range of developmental defects have been reported following exposure to PAHs including pericardial and yolk sac edema, jaw deformities, spinal curvature, and various cardiovascular injuries. Among PAHs, certain congeners proved to be aryl hydrocarbon receptor (AhR) agonists and teratogens with symptoms highly comparable to those of the blue sac disease (BSD) syndrome induced by 2,3,7,8-tetrachlorodibenzo-*p*-dioxin (TCDD) exposure, suggesting

Responsible editor: Markus Hecker

I. Barjhoux · J. Cachot (✉) · P. Gonzalez · H. Budzinski · K. Le Menach · L. Landi · B. Morin · M. Baudrimont
EPOC UMR CNRS 5805, Université de Bordeaux, Avenue des Facultés, 33405 Talence, Cedex,, France
e-mail: j.cachot@epoc.u-bordeaux1.fr

similar modes of action (Barron et al. 2004; Incardona et al. 2004; Brinkworth et al. 2003; Billiard et al. 1999). However, unlike dioxins, PAHs can be rapidly metabolized by vertebrates (Billiard et al. 2008). Indeed, PAHs have the particularity to induce their own metabolization by activating the transcription of genes encoding for phase I drug/xenobiotic cytochrome P450 enzymes, phase II conjugation enzymes, and phase III transporters through AhR pathway activation (Feng et al. 2013; Denison and Heath-Pagliuso 1998). Paradoxically, it is nowadays well established that a variety of unstable and reactive intermediates, sometimes more toxic than the parent compound, as well as reactive oxygen species (ROS) can be generated during PAH metabolism (Shimada 2006; Morel et al. 1999). Consequently, PAHs can exert their developmental toxicity involving a wide range of mechanisms dependent on their chemical structure and rate of metabolization. For instance, Incardona et al. (2004, 2005) reported that primary toxicity of phenanthrene and dibenzothiophene was AhR independent in zebrafish (*Danio rerio*) embryos. In contrast to these congeners but similar to TCDD, the defects in cardiac function and morphogenesis induced by benz[*a*]anthracene proved to be AhR2 dependent and CYP1A independent in zebrafish embryos (Incardona et al. 2006).

The AhR pathway is involved in various signaling pathways covering multiple physiological aspects such as cell proliferation and differentiation, apoptosis, gene regulation, and angiogenesis (Feng et al. 2013). Thus, many AhR-dependent toxic effects of PAHs are likely to result from continuous and inappropriate expression of specific genes in susceptible cells (Denison and Heath-Pagliuso 1998).

Moreover, several enzymes involved in the metabolism of PAHs also participate in the metabolism of retinoids such as CYP1A, UDP-glucoronosyl transferase, and glutathione-S-transferase (Boily et al. 2004). Retinoids are crucial for many vital processes such as growth and development. Both excess and deficiency of retinoids can result in embryotoxicity and/or teratogenicity in vertebrates (Novak et al. 2008). Alteration in retinoid content has also been associated with exposure to PAHs, and the embryotoxic and teratogenic potencies of those compounds make them suspected to interfere with retinoid signaling (Novak et al. 2008; Rolland 2000).

Despite careful analyses and consistent findings across species, the precise mechanisms leading to PAH-associated malformations and sublethal effects in fish ELS are still unclear. In the present study, we propose a modified version of the medaka embryo-larval assay with sediment contact exposure (MELAc) (Barjhoux et al. 2012; Vicquelin et al. 2011) to simultaneously analyze the phenotypic and molecular effects of pyrene (Pyr) and methylpyrene (MePyr) in medaka (*Oryzias latipes*) ELS. Pyr has been found at very high concentrations in sediments, sometimes exceeding 10 μg/g dry weight of sediment (see Table 1) from areas heavily impacted by PAHs. Indeed, Pyr is often among the most abundant of PAHs in sites affected by creosote or pyrogenic inputs (Nagy et al. 2013; Kimbrough and Dickhut 2006; Wang et al. 2001). Moreover, Pyr has been reported to greatly accumulate and to be efficiently metabolized by phase I and phase II enzymes in fish ELS (Honkanen et al. 2008; Petersen and Kristensen 1998). In spite of its weak potency as an AhR agonist (Barron et al. 2004), Pyr exposure induced developmental defects in *D. rerio* embryos that considerably overlap those reported for TCDD (Incardona et al. 2005, 2006). These studies also highlighted the crucial role of CYP1A enzyme activity in the underlying mechanism of Pyr toxicity. MePyr is also present in sediments from PAH-affected areas (Notar et al. 2001). MePyr proved to be bioaccumulable in various aquatic species including teleost fish (Pancirov and Brown 1977) and is considered to be genotoxic and a potent carcinogen in mammals (Glatt et al. 2008; Monien et al. 2008), but to our knowledge, no study is available on the effects of MePyr in fish ELS.

To characterize the potential impact of environmental concentrations of these PAHs in fish ELS, medaka embryos were exposed to Pyr or MePyr-spiked sediments at 300 (C1) and 3,000 (C2) ng/g dry weight (dw) throughout their whole embryonic development. Several noninvasive markers of acute and sublethal toxicity were recorded during the course of the exposure. In parallel, qRT-PCR analysis of transcription levels of target genes was carried out in embryos and newly hatched larvae in order to obtain an overview of the modulations in metabolic pathways following Pyr and MePyr exposure. Finally, the potential genotoxicity of Pyr and MePyr was investigated in 2-day-old larvae using the comet assay.

Material and methods

Experimental design

Japanese medaka (*O. latipes*) embryos of the CAB strain were purchased from GIS Amagen (Gif-sur-Yvette, France). Embryos at 1 day post-fertilization (dpf) were exposed to five different spiked sediments: a control group at 0 ng/g dw of sediment; a Pyr-C1 group at 300 ng Pyr/g dw; a MePyr-C1 group at 300 ng MePyr/g dw; a Pyr-C2 group at 3,000 ng Pyr/g dw; and a MePyr-C2 group at 3,000 ng MePyr/g dw (nominal concentrations). Each treatment consisted of six replicates of 70 embryos each. The first three replicates of each treatment were dedicated to sampling at the embryonic stage (T7) and the three remaining ones kept for larval stage samplings (T9).

Medaka embryos remained in direct contact with the sediment up to sampling time, i.e., for 7 dpf (T7) or up to hatching time (9 dpf, T9), depending on the replicate under consideration. For the duration of the experiment, embryos and larvae

Table 1 Sediment quality guidelines for Pyr in coastal and freshwater sediments and examples of Pyr contamination in sediments for moderately and highly impacted sites

Sediment quality guideline/sampling site	Pyrene concentration (ng/g dw)	Reference
ERL (effect range low)	665	Long et al. (1995)
ERM (effect range medium)	2,600	Long et al. (1995)
TEL (threshold effects level)	153	MacDonald et al. (1996)
PEL (probable effect level)	1,398	MacDonald et al. (1996)
Consensus-based TEC (threshold effect concentration)	195	MacDonald et al. (2000)
Consensus-based PEC (probable effect concentration)	1,520	MacDonald et al. (2000)
Island End River (Boston Harbor, USA)	10,548–42,600[a]	Wang et al. (2001)
Fort Point Channel (Boston Harbor, USA)	1,258–10,042[a]	Wang et al. (2001)
Mystic River (Boston Harbor, USA)	1,694–7,045[a]	Wang et al. (2001)
Industrial discharge area (Cantabrian Sea, Spain)	3,723	Sanchez-Avila et al. (2013)
San Vicente de la Barqueira (Cantabrian Sea, Spain)	319	Sanchez-Avila et al. (2013)
Urdaibai (Cantabrian Sea, Spain)	225	Sanchez-Avila et al. (2013)
Beerkanaal (port of Rotterdam, the Netherlands)	1,130	Heister et al. (2013)
Beneden Merwede River (port of Rotterdam, the Netherlands)	200	Heister et al. (2013)
Mecklenburg Bight dump site (western Baltic Sea, Germany)	224–814[b]	Liehr et al. (2013)
Oissel (Seine Estuary, France)	1,418	Cachot et al. (2006)
La Bouille (Seine Estuary, France)	361–532	Cachot et al. (2006)
Le Havre (Seine Estuary, France)	215	Cachot et al. (2006)

[a] Concentration range measured in different grain size fractions of sediment

[b] Concentration range measured between 2002 and 2004 at the same sampling site

were maintained at 26 °C with a 12 h:12 h photoperiod and under static exposure conditions. After T9 sampling (corresponding to the hatching peak), the remaining embryos and larvae were kept in a clean medium, up to the 11th dpf to assess the genotoxic impact of the exposure on 2 days post-hatching larvae (dph).

Sampled embryos/larvae were divided into pools of adequate size to perform gene expression analysis by qRT-PCR and DNA damage measurement using the comet assay. To complete this genetic aspect of the study, and as described in previous works from our laboratory (Barjhoux et al. 2012; Vicquelin et al. 2011), a wide range of noninvasive phenotypic endpoints were also studied. They included acute toxicity markers such as embryonic survival and hatching success and markers of sublethal effects such as cardiac activity, biometric measurements, time to hatch, and the occurrence and spectrum of developmental abnormalities.

Finally, the time course of Pyr and MePyr contamination was followed in the aqueous phase (i.e., in egg rearing solution, ERS) at T0 (beginning of exposure) and at each sampling time dedicated to molecular analysis (T7 and T9).

Reference sediment characterization

The reference sediment was collected in March 2010 in a pristine gravel pit near Yville-sur-Seine (Seine-Maritime, France). This site has been shown to be marginally contaminated by heavy metals and organic pollutants (Cachot et al. 2006). Moreover, previous studies demonstrated that Yville-sur-Seine sediment is an adequate substrate for medaka embryonic development without any toxic impact on medaka ELS (Vicquelin et al. 2011; Cachot et al. 2007).

The reference sediment was stored at −20 °C, then freeze-dried, and lightly crushed using a mortar and a pestle to eliminate larger particles and homogenize the grain size before use. The physico-chemical characteristics of the sediment were analyzed using the processes described by Barjhoux et al. (2012) and Vicquelin et al. (2011). As shown in Table 2, Yville-sur-Seine sediment can be classified as fine sand with a low carbon organic content. Chemical analyses of this sediment showed a very marginal presence of trace metallic elements and persistent organic pollutants.

Sediment spiking procedure

The freeze-dried (−20 °C at 0.1 mbar for about 48 to 72 h) reference sediment was spiked with Pyr or MePyr to obtain two different nominal concentrations of 300 (C1) and 3,000 ng/g dw (C2) for each compound. The consensus-based probable effect concentration (PEC) established for Pyr by MacDonald et al. (2000; Table 1) was doubled to obtain the C2 nominal concentration. This PEC value was derived from the analysis of sediment quality guidelines published previously and is defined as a threshold concentration above which harmful effects on aquatic organisms are expected to occur frequently (MacDonald et al. 2000). The C2

Table 2 Physico-chemical characteristics of the reference sediment (freeze-dried)

Yville-sur-Seine sediment (Seine-Maritime, Haute-Normandie, France)										
Particulate organic carbon					0.14 %					
Dissolved ammonia (NH_4^+)[a]					40.7 μM					
Dissolved sulfur (H_2S)[a]					17.6 μM					
Grain size distribution										
10th percentile diameter					41.3 μm					
50th percentile diameter					230 μm					
90th percentile diameter					391 μm					
≤65 μm fraction					15.8 %					
Trace metals levels (μg/g dw)										
Co	Mn	Ni	Zn	Cr	As	Ag	Pb	Cd	Cu	
0.74	8.0	1.0	7.3	1.74	0.33	0.01	12.5	0.02	1.09	
Organic compounds levels (ng/g dw)										
Σ PAH[b]					16					
Σ PCB[c]					0.7					
Σ PBDE[d]					Not detected					
Σ OCP[e]					0.1					

[a] Measurements performed on remoistened freeze-dried sediment

[b] Cumulative concentration of 21 analyzed polycyclic aromatic hydrocarbon compounds

[c] Cumulative concentration of eight analyzed polychlorobiphenyl congeners

[d] Cumulative concentration of four analyzed polybrominated diphenylethers

[e] Cumulative concentration of 16 analyzed organochlorine pesticides

concentration can thus be considered as "toxicological"; however, such levels of Pyr contamination can be achieved or exceeded in sediments from some particularly highly contaminated sites (e.g., Boston harbor sediments; Table 1). The C1 concentration was set ten times lower than the C2 concentration. This treatment corresponded to Pyr concentrations that can be measured in contaminated sediments from areas moderately affected by anthropogenic activities (e.g., old waste sites, harbor areas; Table 1). The C1 concentration is also close to the mean threshold effect concentrations (TECs) reported in Table 1 (including ERL, TEL, and consensus-based TEC), below which adverse effects are not expected to occur. In order to compare the toxicity of Pyr and MePyr, the same nominal concentrations were used for both compounds.

The spiking procedure was adapted from the protocol described by Vicquelin et al. (2011). Briefly, an adequate amount of freeze-dried and crushed sediment from Yville-sur-Seine was placed in a 250-mL round-bottomed glass flask and immerged in dichloromethane (DCM, 2 mL/g dw of sediment). Then, 2 mL of isooctane solution containing the required amount of the tested compound (Pyr or MePyr, purchased from Sigma-Aldrich, Lyon, FR) was added to reach the target final concentration. Solvent evaporation was performed using a rotavapor (RV10 Basic, VWR International, Strasbourg, France) equipped with a heating water bath (HB10 Basic, VWR International) set at 45 °C until the sediment was seen to be completely dry. Any potentially remaining traces of organic solvent were eliminated by leaving the sediment overnight at room temperature, in darkness, under an extractor hood. Finally, spiked sediment from each treatment was divided into six aliquots of 12 g dw (for embryo exposure) and one additional aliquot of 5 g dw dedicated to the chemical analysis of Pyr and MePyr.

Medaka embryo exposure

Each aliquot of 12 g dw of spiked sediment was laid in a 55-mm diameter plastic Petri dish and immerged by adding 7 mL of ERS (17.11 mM NaCl; 0.4 mM KCl; 0.36 mM $CaCl_2$; 1.36 mM $MgSO_4$; pH 7.0). The resulting system was then maintained at 26 °C for a 4–5-h equilibration period before the beginning of the experiment. Upon receipt of 24 h post-fertilization (hpf) medaka eggs, healthiness and developmental stage synchronism of the embryos were checked using a stereomicroscope (Leica MZ75, Leica Microsystems, Nanterre, France) and cold light source (Intralux® 4100, Volpi AG, Schlieren, Switzerland). Immediately after sorting, 70 embryos per replicate (six replicates per treatment) were randomly placed on a Nytex® mesh (mesh opening 1,000 μm, Sefar Filtration Inc., Depew, NY, USA). The Nytex® grid was then slightly sunk into the sediment. Afterwards, embryos remained exposed to the sediment in a climate cabinet (Economic Delux, Snijders Scientific, Tilburg, Netherlands) at 26±0.3 °C with a 12-h:12-h photoperiod (5,000 lx white light) until hatching time (9 dpf) and then placed in clean ERS medium up to the end of experiment at 11 dpf (comet assay performed on 2-day-old larvae). The remaining embryos or larvae were euthanized using MS222 (Sigma-Aldrich) solution at 1 g/L. During the exposure period, the level of ERS was checked daily and readjusted in case of evaporation. Dissolved oxygen was also checked daily at the water-sediment interface using an oxygen optical microsensor (NeoFox® Foxy probe, Ocean Optics sensors, IDIL Fibres optiques, Lannion, France). This measurement confirmed good oxygenation of the medium with values always higher than 80 % saturation (data not shown).

Phenotypical endpoints

The different procedures performed for phenotypic endpoint assessments have been previously detailed by Barjhoux et al. (2012). Viability was checked daily for all individuals and all conditions. Cardiac activity was monitored in 6 and 7 dpf embryos (five randomly selected individuals per replicate). Biometric measurements (total body length, head size, and

head/body length ratio) and developmental anomalies (spinal, craniofacial, ocular, cardiovascular, yolk sac, and edema) were observed in 15 randomly selected newly hatched larvae per replicate. All these observations were done in an air-conditioned room at 23±1 °C using a stereomicroscope (MZ75, Leica Microsystem) equipped with a color CCD camera (Leica DFC 420C), connected to an image analysis software program (Leica Application Suite v2.8.1.) and a cold light source (Intralux® 4100, Volpi AG).

Gene transcription analysis

Gene expression analysis was conducted on three samples of eight pooled individuals per replicate and on three replicates per treatment at each sampling time (T7 and T9). A panel of 12 genes was selected for transcriptional analysis due to their involvement in xenobiotic metabolism, antioxidant defenses, mitochondrial metabolism, DNA repair, cell cycle regulation, and apoptosis. The response to oxidative stress was studied through cytoplasmic (*sod*(*Cu*/*Zn*)) and mitochondrial superoxide dismutase (*sod*(*Mn*)) gene transcription. Activation of Pyr and MePyr phase I metabolism was studied through *cyp1A* gene transcription. The impact of Pyr and MePyr on the mitochondrial electron transport chain was investigated using cytochrome C oxidase subunit I (*coxI*) transcripts. The *ogg1* (8-oxoguanine glycosylase 1) was selected for its involvement in oxidative DNA damage repair. PAH-induced apoptosis was studied through Bcl-2-associated X protein (*bax*) and *p53* gene transcription levels. The wingless integration site 1 (*wnt1*) gene was also selected for its key role in cell differentiation and proliferation. Finally, four genes involved in retinoid metabolism (retinaldehyde dehydrogenase type 2, *raldh2*) and retinoic acid signaling pathway (retinoic acid receptor alpha 1, *rarα1*; retinoic acid receptor gamma 1, *rarγ1*; retinoid X receptor, *rxrα1*) were also studied.

Each pool of embryos or larvae was entirely immerged in RNAse-free microtubes containing 200 μL RNA Later® (Qiagen, Manchester, UK) and quickly frozen by dipping in liquid nitrogen. Samples were then stored at −80 °C until RNA extraction.

Total RNA extraction was performed using the Absolutely RNA® Miniprep kit (Agilent Technologies France SAS, Les Ulis, France) according to the manufacturer's instructions, with an additional phenol-chloroform-isoamylic alcohol (25:24:1, *v*/*v*) purification step. The quality and the quantity of the extracted RNA were determined by spectrophotometry at 260 and 280 nm.

First-strand complementary DNA (cDNA) was synthesized using the Affinity Script™ Multiple temperature cDNA Synthesis kits (Agilent). Briefly, 1 μL of oligo dT (1 μM), 1 μL of random primers (1 μM), 0.8 μL of dNTPs (10 mM), and 2 μL of AffinityScript™ RT buffer (10×) were mixed together with 14 μL of the previously extracted RNA (approximately 5 μg). The mixture was then incubated in a thermocycler (MasterCycler pro™, Eppendorf, Le Pecq, France) for 5 min at 65 °C. cDNA synthesis was performed by adding 1 μL of reverse transcriptase (1 U) and 0.5 μL of RNase block ribonuclease inhibitor (0.5 U) and then by incubating the mixture at 42 °C for 1 h. cDNA samples were then stored at −20 °C until quantitative real-time PCR was performed.

The coding sequences of the 13 selected genes (Table 3) were obtained from the GenBank (PubMed–NCBI) and HGNC (Ensembl, EMBL–EBI) databases. The accession number of each coding sequence is reported in Table 3. For each gene, specific primer pairs were determined using the LightCycler probe design software (v1.0, Roche, Meylan, France) and are mentioned in Table 3. Primers were purchased from Sigma-Aldrich (Easy Oligo™).

The amplification of cDNA was monitored using the fluorescent DNA binding dye SyberGreen I. Real-time PCR reactions were performed using an Mx3000P™ system (Stratagene, Agilent) and Brilliant III Ultra-Fast SYBR® Green QPCR Master Mix kits (Agilent) according to the manufacturer's instructions.

PCR reactions were prepared in 96-well microplates adding 10 μL of SYBR® Green QPCR master mix (2×), 7 μL of ultra-pure water (nuclease-free PCR-grade water), 2 μL of primer pair mix (2 μM), and 1 μL of cDNA. Afterwards, PCR reactions consisted of an activation cycle (10 min at 95 °C) followed by 50 amplification cycles (30 s at 95 °C, 40 s at 60 °C, and 30 s at 72 °C).

The specificity of each amplification cycle was determined from the dissociation curve of the PCR product. These dissociation curves were obtained by following the SyberGreen fluorescence level during a gradual heating of the PCR products from 65 to 95 °C (0.1 °C/s). Relative quantification of each gene transcription level was normalized according to β-*actin* and *rpl7* genes using the $2^{-\Delta Ct}$ method described by Livak and Schmittgen (2001), where ΔCt represents the difference between the cycle threshold (Ct) of a specific gene and the mean Ct of the housekeeping genes (β-*actin* and *rpl7* genes in the present study).

Comet assay

DNA damage induced by Pyr and MePyr exposure was evaluated on a pool of five 2 dph larvae (one pool sampled per replicate on three replicates per treatment) using the comet assay. Cell dissociation and comet assay procedures were carried out following the protocol of Morin et al. (2011). Briefly, pools of larvae were digested in a MEM-Collagenase IV 0.125 % (*w*/*v*) medium, and cell viability was checked using a trypan blue exclusion test (only cell suspensions with viability superior to 80 % were used). Once embedded in a 1 %

Table 3 Accession number and sequence of primer pairs for the thirteen *O. latipes* genes used in the present study

Gene	Function	Accession number (EMBL or GenBank)	Primers sequences
β-*actin*	Cytoskeletal gene (housekeeping gene)	S74868	GTGACCCACACAGTGCC[a] GCGACGTAGCACAGCTTC[b]
rpl7	Ribosomal protein L7 (housekeeping gene)	NM_001104870	AACGTGGCTACGGCAG[a] CGAGGTGACGACAGCTT[b]
coxI	Cytochrome c oxidase subunit I (complex IV of the mitochondrial respiratory channel)	NC_004387 (gene ID 805432)	TTCCCCCAACACTTCTTAGGC[a] TGTGGCTGTTAGTTCGACTGA[b]
p53	Tumor suppressor gene P53	AF212997	TCTGGCACTGCAAAGTCTGT[a] CCTCGTTTTGGTGGTGGG[b]
cyp1a	Cytochrome P450 1A	AY297923	CTCCCTTTCACAATTCCACACT[a] TGCAACGCCGCTTTCC[b]
wnt1	Wingless integration site 1 (cell proliferation and somitogenesis)	AJ243208	CCGCTTTGACGGAGCAT[a] TTGAACCCACGCCCACAGC[b]
sod(*Mn*)	Mitochondrial Fe/Mn superoxide dismutase	ENSORLG00000013261	ATGGCTGGGCTATGACAAAG[a] TGGCTATCTGAAGACGCTCAC[b]
sod(*Cu*/*Zn*)	Cytosolic Cu/Zn superoxide dismutase	ENSORLG00000008041	GGGAAATGTGACCGCAGG[a] GCCAAACGCGCTCCAG[b]
bax	Bcl-2-associated X protein gene	ENSORLG0000000456	TCTTCGCTCAGTCCCTCC[a] GCCAACGTCTGCCAGCCA[b]
ogg1	8-Oxoguanine glycosylase 1 gene (BER family)	ENSORLG00000010758	CTCGTATTCAGGGCATGGT[a] ACCCGTGGCTGTCTAAG[b]
raldh2	Retinaldehyde dehydrogenase type 2	NM_001104821	GCCGCTCACCTGTCTCTAT[a] TCCCTGCCGCCTCTTG[b]
rarα1	Retinoic acid receptor alpha 1	EF546452	GCATCATCAAGACGGTGGAG[a] GGCGAAAGCGAAAACCAGG[b]
rarγ1	Retinoic acid receptor gamma 1	EF546454	CTCGTGTCTACAAACCCTGC[a] ATGCCGACCTCGAAGC[b]
rxrα1	Retinoid X receptor alpha 1	EF537036	GGGTGCCTTCGAGCCA[a] CCGGTAACCGCAGCAACAGT[b]

[a] Upstream primer

[b] Forward primer

low melting point agarose gel, cells were lysed (2.5 M NaCl, 0.1 M EDTA, 0.01 M Tris; pH=10; at 4 °C for 1 h) and immerged in an electrophoresis buffer (0.3 M NaOH, 1 mM EDTA; pH>13) for 15 min to allow the DNA to unwind. Then, electrophoresis was carried out at 25 V, 300 mA for 15 min (1 V/cm). Ethidium bromide (20 mg/L) was used as DNA fluorescent tag and all coded slides were randomly analyzed for 75 nuclei per gel (two gels per experimental replicate) using an Olympus epi-fluorescent microscope (×400 magnification) equipped with a grayscale CCD camera (Zeiss, DE) and the Komet 5.5 software program (Kinetic Imaging, Liverpool, UK). As recommended by Hartmann et al. (2003), % tail DNA (percentage of DNA which migrates from the nucleus, i.e., the head of the comet) was the selected parameter used for the measurement of DNA damage. Heavily DNA-damaged nuclei displaying a small or inexistent head and a large diffuse tail, known as "hedgehog cells," were not taken into account in the comet measurement, according to the recommendations of Kumaravel et al. (2009). However, the percentage of hedgehog cells, which have also been reported as apoptotic or necrotic cells (Olive and Banath 1995), was visually scored on a total of 100 cells per gel.

Pyr and MePyr analysis

Sediment analysis

Pyr and MePyr extraction and analysis were performed according to the procedures described in previous studies (Devier et al. 2005; Letellier et al. 1999). In brief, spiked sediments were extracted using microwave-assisted extraction (30 W for 10 min, in a Maxidigest 350, ProLabo, Fontenay-sous-Bois, France) with 30 mL of DCM and 30 μL of β-mercapto ethanol. Depending on the expected PAH concentration, the extracted quantity of freeze-dried sediment varied from 0.5 g (for C2 treatments) and 1 g dw (control sediment and C1 spiking level). One extraction blank (complete procedure without matrix) was included in each series of extraction. Deuterated fluoranthene (Fluod10) was used as an internal

standard and gravimetrically added prior to the extraction procedure in each sample and blank.

After extraction, the samples were reconcentrated using a Vacuum Evaporation System (RapidVap, Labconco, Fort Scott, KS, USA; 900 mbar, 50 °C). The concentrated extracts were then purified on a microcolumn containing activated copper and alumina and reconcentrated in isooctane. Afterwards, purified samples were loaded onto a microcolumn containing silica. The aliphatic fraction was discarded by elution with pentane, whereas the aromatic fraction containing the PAHs was subsequently eluted with a mixture of DCM-pentane (65:35 *v*/*v*). The aromatic extracts were reconcentrated in DCM and analyzed using gas chromatography-mass spectrometry (GC/MS). Deuterated pyrene (Pyr10) was used as syringe standard and gravimetrically added to each extract and blank just before injection.

The accuracy and the validity of the quantification method were tested during each analysis series using two standard solutions containing known amounts of Pyr, MePyr, and deuterated standards (Fluod10 and Pyr10). The first standard solution was used to evaluate the response factors (Pyr/Fluod10, MePyr/Fluod10, and Fluod10/Pyr10). The second independent standard solution was used to test the efficiency of the quantification method, which varied between 103 and 105 % for Pyr, between 100 and 101 % for MePyr, and between 98 and 99 % for Fluod10.

Aqueous phase analysis

At each sampling time, approximately 4 mL of ERS was sampled from three replicates and pooled together for the same treatment (except for T0 sampling for which 20 mL of clean ERS was analyzed). Aqueous samples were separated from sediment particles with a 15-min centrifugation at 3,500 *g* at 15 °C and stored at −20 °C in the dark until analysis.

Pyr and MePyr extraction was performed by solid phase microextraction (SPME) and analyzed by GC/MS as described by de Perre et al. (2014). The same internal and syringe standards as mentioned for sediment analysis were used. The efficiency of the quantification method has been evaluated to be 116 % for Pyr and 126 % for MePyr.

Statistical analysis

The data is expressed as mean ± standard deviation (SD). Statistical analyses were conducted using Statistica 7.1 software (Statsoft, Maisons-Alfort, France). Results were initially tested for normality (Shapiro-Wilk's test on residues with 1 % risk) and homoscedasticity (Levene's test, 5 % risk). When necessary, data was transformed to fulfill normality and homoscedasticity criteria. Afterwards, significant differences between treatments were tested with a one-way or two-way ANOVA analysis followed by post hoc Tukey's test ($p<0.05$). If data transformation was not sufficient to perform parametric analysis, then the nonparametric Kruskall-Wallis' test followed by Bonferroni-Dunn's post hoc test was used ($p<0.05$). Finally, relative gene transcription data was statistically analyzed using *t* test for independent samples (only pairing comparisons with the control treatment were performed).

Results and discussion

In previous studies, the MELAc proved to be a reliable, sensitive, and integrative bioassay specifically designed for toxicity assessment of sediment-bound chemicals including metals and hydrophobic substances (Barjhoux et al. 2012; Vicquelin et al. 2011). The present work proposes an adaptation of this assay for a combined analysis of embryotoxicity, teratogenicity, and genetic disturbances induced by Pyr and MePyr in medaka ELS. During the time course of the exposure to spiked sediments, several phenotypical and noninvasive markers of toxicity and embryonic development impairment were investigated in embryos and larvae. This approach was completed by the analysis of target gene transcription levels by qRT-PCR and DNA damage measurement using the comet assay.

Pyr and MePyr contamination in the spiked sediments and the water column

Chemical analysis revealed a clear concentration-dependent increase of Pyr and MePyr content in Pyr- and MePyr-spiked sediments, respectively (Table 4). The spiking efficiencies, calculated by comparison between Pyr or MePyr contents in sediment at T0 and the expected concentration based on the amount of compound introduced during the spiking procedure, were satisfying and varied between 83 and 92 % for Pyr and between 70 and 88 % for MePyr. The resulting exposure concentrations in sediments were close to the targeted values.

Pyr and MePyr concentrations in the aqueous phase of the control treatment were low and varied from 1.48 to 12.5 ng/L for Pyr and from 0.16 to 3.5 ng/L for MePyr (Table 4). Pyr concentration in the ERS buffer from the different treatments showed a trend of increasing over the time course of the experiment to reach maximal values of 629 and 3,125 ng/L at T9 in C1 and C2 treatments, respectively. The same tendency was observed for the MePyr-C2 treatment for which MePyr concentration peaked at 1,831 ng/L at the end of exposure. Surprisingly, the aqueous phase from the MePyr-C1 treatment was more contaminated by MePyr at T7 (98.3 ng/L) than at T9 (53.5 ng/L) (Table 4). The contamination of the water column is probably due to the desorption of Pyr or MePyr labile fraction from the sediment particles and the diffusion of these compounds from the sediment pore

Table 4 Pyr and MePyr concentrations in spiked sediments and ERS buffer at T0 (beginning of exposure), T7 (7 dpf), and T9 (9 dpf) sampling times

Condition	Pyrene			Methylpyrene			Nominal concentration	Spiking efficiency (%)[a]
	T0	T7	T9	T0	T7	T9		
Concentration in sediment (ng/g dw)								
Control	<0.1	–	–	<0.1	–	–	0	
Pyr-C1	250	–	–	<0.1	–	–	300	82.8
Pyr-C2	2,770	–	–	<0.1	–	–	3,000	92.1
MePyr-C1	62	–	–	202	–	–	300	69.7
MePyr-C2	<0.1	–	–	2,586	–	–	3,000	87.8
Concentration in ERS buffer (ng/L)								
Control	1.48	12.5	3.17	0.16	0.39	3.50		
Pyr-C1	–	204	629	–	0.12	1.17		
Pyr-C2	–	2,488	3,125	–	0.19	1.10		
MePyr-C1	–	8.02	58.4	–	98.3	53.5		
MePyr-C2	–	9.56	5.21	–	1,698	1,831		

[a] Spiking efficiency calculation was based on the exact amount of Pyr or MePyr introduced during the spiking procedure

water. According to some authors, the bioavailability of PAHs (and thus, toxicity) is highly governed by their concentration in the aqueous phase and, more particularly, in the pore water of contaminated soils or sediments (Geffard et al. 2003; Sverdrup et al. 2002). In the present work, measured concentrations of Pyr and MePyr in the ERS buffer were relatively low and only reached a few micrograms per liter in the most highly contaminated treatments. However, it can be hypothesized that dissolved PAHs may have been locally more concentrated in sediment pore water during the exposure. Sverdrup et al. (2002) proposed a method for the calculation of PAH concentration in pore water as a function of PAH content in spiked sediments and their soil organic carbon-water partitioning coefficient (K_{oc}). When applied to Pyr and MePyr sediment contents measured in the present work, concentrations in pore water could reach 2.7 and 30 μg/L for Pyr and 1.16 and 14.9 μg/L for MePyr, for C1 and C2 treatments, respectively (calculations carried out using an *n*-octanol-water partitioning coefficient, log K_{ow}, equals to 5.2 for Pyr according to Sverdrup et al. (2002) and to 5.48 for MePyr as predicted by US-EPA EPI suite™). Concentrations measured in the aqueous phase at the end of the exposure were well below these predicted values.

Only Pyr induces low mortality in embryos exposed to spiked sediments

MePyr exposure did not induce any significant impact on survival rate in exposed embryos; the mean viability was above 95 % in both treatments (Table 5). Conversely, Pyr exposure resulted in a slight concentration-dependent reduction of embryos survival, which was significant for the Pyr-C2 concentration when compared to the control ($p<0.03$). However, mean embryonic survival in this treatment remained high (>90 %) and only represented a decline of 5 % in comparison to the unexposed embryos (Table 5).

According to these observations and considering that only dissolved PAHs are biologically available for fish embryos (Carls et al. 2008), a lethality threshold of 3 μg/L of Pyr in the water column can be established for medaka embryos exposed to spiked sediment. These results are in agreement with the lowest observed effect concentration (LOEC) value of 2.5 μg/L reported for the survival of turbot larvae (*Psetta maxima*) exposed to Pyr during 96 h (Mhadhbi et al. 2010). Li et al. (2011) also observed a 5 to 10 % mortality in *Sebastiscus marmoratus* larvae exposed to 1 μg/L of Pyr. On the contrary, *Cyprinodon variegatus* exposure to 20 μg/L of Pyr did not induce significant reduction of the embryonic survival rate (Hendon et al. 2008). It has also been reported that Pyr-induced lethality following embryonic exposure mainly occurred at the larval stage, several days after hatching (Hendon et al. 2008; Incardona et al. 2004). It is thus possible that additional mortality could occur in medaka ELS if the exposure was prolonged later at the larval stage. Based on the above mentioned data, it seems that medaka ELS have similar sensitivity to *P. maxima* larvae but are clearly more sensitive than *C. variegatus* embryos when exposed to Pyr in the water column. Nonetheless, it must be emphasized that, as discussed above (see "Pyr and MePyr contamination in the spiked sediments and the water column"), Pyr could be more concentrated in sediment pore water (up to 30 μg/L, according to the calculation method of Sverdrup et al. (2002)), thus leading to higher exposure concentrations when fish embryos develop at the surface or in the sediment. Additionally, other studies suggested that particle-bound PAHs could also contribute to the toxic effects acting as a secondary source of

Table 5 Embryonic survival, hatching success, and time to hatch following exposure of medaka embryos to Pyr or MePyr-spiked sediments

Condition	Embryonic survival (%)	Hatching success (%)	Time to hatch (dpf)
Control	96.7±2.24 a	87.0±8.74 a	9.50±0.26 a
Pyr-C1	94.0±4.40 a,b	77.2±1.04 a,b	9.82±0.01 a,b
Pyr-C2	91.6±1.33 b	71.4±14.4 a,b	9.87±0.57 a,b
MePyr-C1	96.0±2.35 a,b	46.1±17.0 b	10.8±0.39 b
MePyr-C2	95.6±2.58 a,b	80.3±12.1 a,b	9.70±0.1144 a,b

Values represent the mean responses (±SD) from six replicates for embryonic survival and from three replicates for hatching success and time to hatch. For time to hatch calculations, the hatching day of unhatched embryos at the end of experiment was set at 12 dpf. Different letters indicate significant differences between treatments using one-way ANOVA followed by Tukey's post hoc test ($p<0.05$; degree of freedom (df) = 4)

contamination in embryos exposed to contaminated sediments (Hollert et al. 2003; Kocan et al. 1996). Consequently, it seems relevant to specify Pyr concentrations in sediment when establishing toxicity threshold values using a sediment contact bioassay. The present study thus revealed the relatively low acute toxicity of Pyr in medaka embryos with a lethality threshold equal to 2.8 μg/g dw in the sediment and 3 μg/L of Pyr in the water column.

Pyr and MePyr impact in ovo development of medaka embryos

Hatching success and time to hatch of embryos was recorded over a 11-dpf period (Table 5). However not significant, a concentration-dependent decrease of hatching success was observed following Pyr exposure, down to 71 % for the C2 treatment. The mean time to hatch in Pyr-exposed treatments was consistently delayed in a concentration-dependent way although not significantly different from the control treatment ($p>0.05$ according to ANOVA results followed by Tukey's post hoc test; Table 5). Only 46 % of the embryos exposed to MePyr-C1 concentration hatched during the 11-dpf period which resulted in a mean time to hatch of 10.8 dpf for this treatment (Table 5). This significant ($p<0.05$) impairment of the hatching success and the time to hatch in comparison to the control indicates that medaka embryonic development was noticeably delayed/halted by MePyr at concentrations of 202 ng/g dw in sediment and up to 98 μg/L in the water column. Surprisingly, exposure to the highest concentration of MePyr did not noticeably impact hatching success. It could be interpreted as a hormetic effect of MePyr exposure on hatching events. However, further experiments are needed using a wider concentration range of MePyr to conclude.

Medaka in ovo growth was evaluated through biometric measurement acquisition on newly hatched larvae. Results showed a concentration-dependent reduction of larvae total body length following exposure to both Pyr and MePyr (Fig. 1). On average, larvae exposed to C2 treatments were significantly 4 and 5 % shorter than control larvae in Pyr and MePyr treatments, respectively ($p<0.02$ for Pyr and $p<0.01$ for MePyr). Nevertheless, no significant effect of Pyr and MePyr was highlighted on the average head size of newly hatched larvae (Fig. 1) or on head/body length ratio (data not shown). As a result, analysis of general in ovo development endpoints (including hatching success, time to hatch, and larval length) demonstrated that Pyr significantly altered medaka growth at the highest concentration (2.8 μg/g dw of sediment and up to 3.1 μg/L in the aqueous phase) and that MePyr impacted embryonic development from the lowest concentration tested (0.2 μg/g dw of sediment and up to 0.1 μg/L in the aqueous phase).

A concentration-dependent inhibition of hatching success was reported in *P. maxima* embryos exposed to Pyr from 1.25 to 40 μg/L (Mhadhbi et al. 2010). Hatching rate (but not time to hatch) was also significantly reduced in *C. variegatus* embryos exposed to 150 μg/L of Pyr and 18 dpf larvae showed a reduced body length following exposure to 20 μg/L (Hendon et al. 2008). Likewise, Rhodes et al. (2005) reported a strong reduction of hatching success and larval hatching length in medaka ELS exposed to an environmental extract characterized by a high content of alkyl-PAH. The authors assumed that

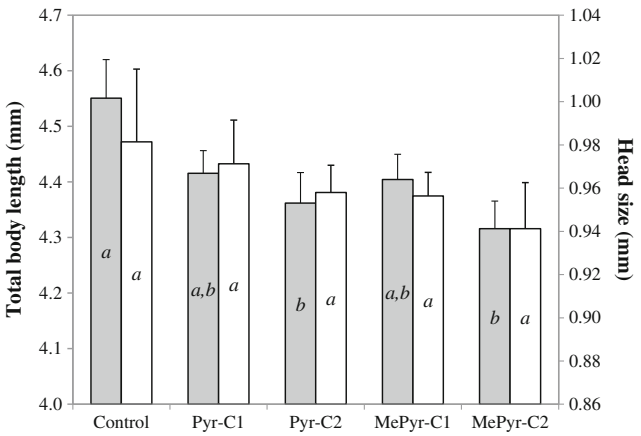

Fig. 1 Total body length (*gray bars*) and head size (*white bars*) of medaka larvae at hatching following exposure to Pyr- or MePyr-spiked sediments. Values represent the mean response (±SD) from three replicates. *Different letters* indicate significant differences between treatments using one-way ANOVA followed by Tukey's post hoc test ($p<0.05$; $df=4$)

PAH metabolites could impair energy metabolism resulting in an inhibition of hatching success since escaping the chorion is highly energy dependent. It could also be suggested that PAH biotransformation is energy-consuming, therefore limiting the energy store available for growth and hatching. These hypotheses are thus coherent with reduced growth (i.e., larval length) of newly hatched medaka larvae following exposure to environmental PAH extracts (Farwell et al. 2006; Rhodes et al. 2005) and to Pyr and MePyr in the present work. However, other observations seem to indicate that the reduction of larva body size following PAH exposure is linked to the decreased absorption of yolk due to cardiovascular dysfunction (Billiard et al. 1999; see "*Pyr and MePyr exposure strongly affects the cardiovascular system of embryos*" for details).

Pyr and MePyr are highly teratogenic in medaka ELS

Observations of developmental abnormalities in newly hatched medaka larvae following embryonic exposure to spiked sediments revealed the high teratogenic potency of both Pyr and MePyr. A significant ($p<0.001$, when compared to the control) and dramatic increase of the percentage of abnormal larvae, above 80 % in all treatments, was observed from the lowest concentrations of Pyr and MePyr (Fig. 2). Such high percentages of affected larvae have been reported in medaka ELS exposed to phenanthrene and alkylphenanthrenes up to 1,000 μg/L (Turcotte et al. 2011) and in *C. variegatus* larvae following exposure to 150 μg/L of Pyr (Hendon et al. 2008).

In the present study, exposed larvae were significantly affected by cardiovascular impairments (at all tested concentrations of Pyr and MePyr), spinal deformities (in the MePyr-C2 treatment), yolk sac resorption defects (in both Pyr treatments and at the highest concentration of MePyr), and craniofacial abnormalities (in the Pyr-C2 treatment) in comparison to the control group (Fig. 2). Most of these developmental abnormalities have already been described in fish ELS following exposure to Pyr (Li et al. 2011; Mhadhbi et al. 2010; Incardona et al. 2004). Interestingly, many of these defects have also been observed in fish ELS exposed to TCDD (Antkiewicz et al. 2005; Hornung et al. 1999; Elonen et al. 1998) and are often assimilated to BSD symptoms.

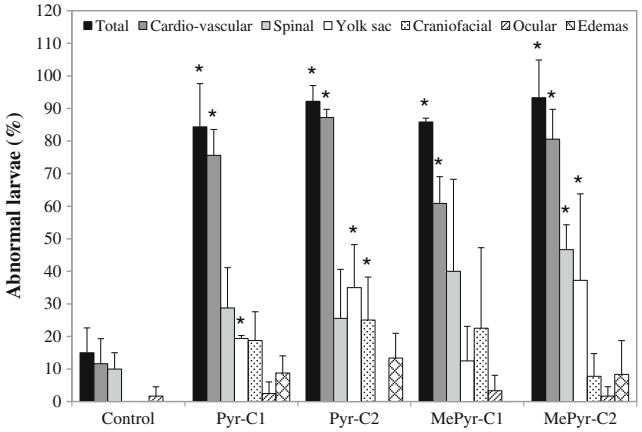

Fig. 2 Developmental abnormalities in newly hatched larvae following Pyr or MePyr exposure. Values represent the mean response (±SD) for three replicates. Statistical analysis was performed on each endpoint independently. *Asterisks* indicate significant differences in comparison with the control according to the results of one-way ANOVA followed by Tukey's post hoc test ($p<0.05$; $df=4$) or nonparametric Kruskall-Wallis ANOVA followed by Bonferroni-Dunn's post hoc test ($p<0.05$; $df=4$) for craniofacial deformities

Pyr and MePyr exposure strongly affects the cardiovascular system of embryos

The cardiovascular system is known to be particularly sensitive to PAH exposure in fish ELS (Carls et al. 2008; Incardona et al. 2004). In the present study, Pyr and MePyr exposure did not significantly affect cardiac activity in 6 and 7 dpf embryos (data not shown). However, PAH exposure induced a significant concentration-dependent increase of the percentage of larvae showing cardiovascular injuries in all exposed treatments in comparison to the control (Fig. 2). This kind of developmental defect was the most frequently observed and affected 76 to 87 % of the larvae exposed to Pyr and 61 to 81 % of the larvae from MePyr treatments. These impairments included abnormal positioning of the heart chambers in relation to each other and to the cephalo-caudal axis as well as heart hypo-, hyper-, or dystrophies.

Antkiewicz et al. (2005) also observed altered heart looping resulting in abnormal relative positioning of the heart chambers, hypo- and dystrophy of the heart chambers in zebrafish embryos exposed to TCDD. Heart morphology impairments were associated with cardiac dysfunction and/or vascular circulatory defects, even if both cause and effect relationship remained possible (Antkiewicz et al. 2005).

Similarities between Pyr and TCDD cardiotoxicity have been already reported in zebrafish ELS (Incardona et al. 2004, 2006). However, in this species, Pyr mainly induced anemia syndrome, reduced vascular peripheral circulation, and caused pericardial and yolk sac edemas (Incardona et al. 2004). Interestingly, exposure of *D. rerio* embryos to phenanthrene and benzo[*a*]anthracene caused the appearance of similar cardiovascular pathologies as described by Antkiewicz et al. (2005) and the present study.

Although not significant, pericardial edemas were observed in larvae following exposure to both Pyr treatments (9 to 13 %) and MePyr-C2 concentration (8 %; Fig. 2) with a p value close to significance threshold for Pyr-C2 treatment ($p=0.06$). Similar observations were reported in *C. variegatus* larvae exposed to 150 μg/L of Pyr (Hendon et al. 2008). According to Billiard et al. (1999), the appearance of edemas in rainbow trout and zebrafish larvae exposed to retene

suggested leakiness of the endothelial vasculature and may be an overt sign of cardiovascular dysfunction. Considering that the vitelline vessels supplying yolk to the embryo are critical for absorption of yolk nutriments, loss of vascular integrity could interfere with release of yolk metabolites to vitelline circulation (Billiard et al. 1999). In the present study, reduced yolk absorption was significantly induced in a concentration-dependent way in newly hatched larvae exposed to both Pyr treatments and to MePyr-C2 treatment, in comparison to the control group ($p<0.05$; Fig. 2). As described above, these effects were concomitant to a decrease of larval body length and cardiovascular injuries in larvae exposed to Pyr and MePyr-C2 treatments. Moreover, cardiovascular dysfunction has been linked with decreased absorption of the yolk sac in medaka ELS exposed to TCDD (Elonen et al. 1998). All these observations suggest that Pyr and MePyr-induced inhibition of growth is the consequence of yolk malabsorption in exposed larvae, as a result of cardiovascular dysfunctioning, as previously suggested for TCDD (Antkiewicz et al. 2005; Elonen et al. 1998). The reduced vascular peripheral circulation observed in *D. rerio* early larval stage exposed to Pyr (Incardona et al. 2004, 2006) seems to corroborate this hypothesis.

Induction of skeletal deformities following embryonic exposure to Pyr and MePyr

Although cardiovascular injuries were the main developmental abnormalities induced by Pyr and MePyr exposure, different skeletal deformities were also recorded in exposed larvae at hatching. Indeed, 26 to 29 % of Pyr-exposed larvae and 40 to 47 % of MePyr-exposed larvae ($p<0.05$ for MePyr-C2 treatment when compared to the control, according to one-way ANOVA followed by Tukey's post hoc test) showed abnormal spinal curvature including lordosis, kyphosis, and C-shaped larvae (Figs. 2 and 3). Additionally, 19 and 25 % of the larvae exposed to Pyr-C1 and Pyr-C2 treatments, respectively, showed craniofacial abnormalities primarily in the lower jaw (Fig. 2, $p=0.053$ and $p<0.05$, respectively). Similar developmental impairments were also noticeable in 23 % of larvae from MePyr-C1 treatment ($p=0.053$ in comparison to the control; Fig. 2).

Comparable spinal and jaw deformities have been reported in several fish larvae following exposure to Pyr (Li et al. 2011; Hendon et al. 2008; Incardona et al. 2006). Such developmental defects were also induced in fish ELS exposed to TCDD (Teraoka et al. 2002, 2006; Elonen et al. 1998). The concomitant induction of CYP1A (at the protein and messenger RNA (mRNA) levels) and occurrence of skeletal defects in *C. variegatus* and *D. rerio* larvae suggested that the CYP1A pathway is involved in the development of spinal deformities in Pyr-exposed organisms (Hendon et al. 2008; Incardona et al. 2006). Moreover, spinal deformities (mainly kyphosis or lordosis) were reported in Pacific herring (*Clupea pallasi*) larvae following exposure to weathered crude oil (Carls et al. 1999). The authors also noticed that deformed larvae showed difficulties to swim normally and that spinal curvature was the most important predictor of swimming ability. As reduced swimming ability may also impact upon prey capture capacity or predator escape performance, these observations suggested that additional mortality could occur in heavily affected individuals after complete resorption of yolk reserves.

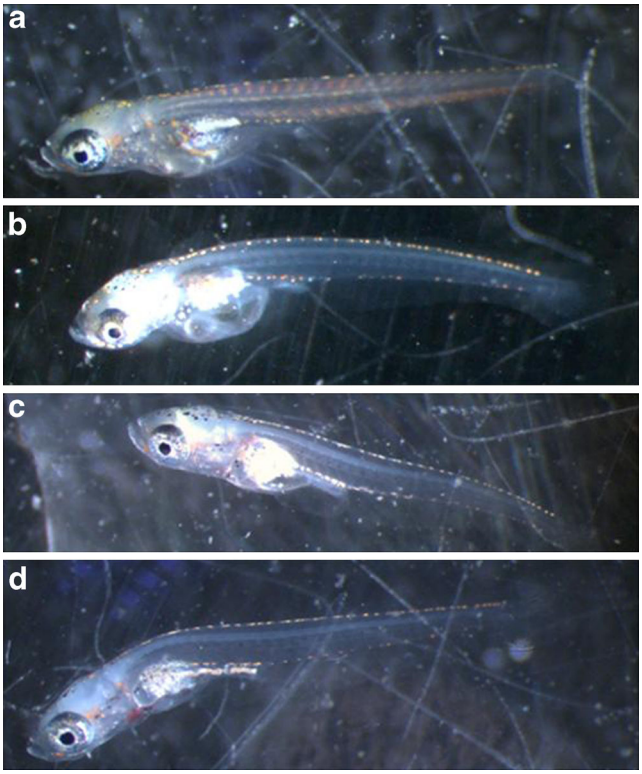

Fig. 3 Examples of spinal deformities observed in newly hatched larvae following Pyr or MePyr exposure. **a** Normal larvae from control treatment; **b** C-shaped larvae following Pyr-C1 exposure; **c** larvae showing lordosis and **d** kyphosis following MePyr-C2 exposure

Wnt-1 signaling pathway is highly implicated in embryogenesis and morphogenesis through cell differentiation and proliferation control (L'Allemain 2006). In particular, Wnt signaling (including Wnt-1 members) is involved in the dorso-ventral patterning of the spinal cord, promoting dorsal identities in combination to Sonic hedgehog (Shh) pathway which induces ventral ones (Ulloa and Marti 2010). Several lines of evidence indicate that antagonist interactions between these two signaling pathways, highly conserved through evolution, would define the dorso-ventral patterning of the developing central nervous system and direct myotome formation (Ulloa and Marti 2010; Münsterberg et al. 1995). In the present study, *wnt1* transcription level was significantly increased in comparison to the control in medaka larvae following exposure to Pyr-C1 treatment ($p<0.05$) and both MePyr concentrations ($p<0.01$, Table 6). Supporting these

Table 6 Variations in differential gene transcription levels as compared to the control observed in medaka embryos (T7) and larvae (T9) after exposure to Pyr- or MePyr-spiked sediments

	Mitochondrial metabolism	Xenobiotic metabolism	Oxidative stress defense		Cell cycle arrest/apoptosis		Development/ embryogenesis	DNA repair	Retinoid metabolism			
	cox I	*cyp1a*	*sod*(*Mn*)	*sod*(*Cu*/*Zn*)	*p53*	*bax*	*wnt1*	*ogg1*	*raldh2*	*rarα1*	*rarγ1*	*rxrα1*
Embryonic stage (T7)												
Pyr-C1	1.1	1.0	1.0	0.9	1.1	0.8	1.0	0.9	0.8	1.3	0.8	1.1
Pyr-C2	1.5*	1.8*	1.1	1.0	1.2	1.4	1.8	1.2	0.8	1.5	1.0	2.0[a]
MePyr-C1	1.4*	1.1	1.1	1.0	1.4	0.9	0.8	1.0	0.7	1.4	0.8	1.5
MePyr-C2	1.7*	2.5*	1.1	1.0	1.3	1.1	1.7	2.1	1.0	1.8*	1.1	2.0
Larval stage (T9)												
Pyr-C1	0.9	1.7	1.1	0.8	1.4	0.9	2.6*	1.1	1.4	1.5	1.0	1.2
Pyr-C2	0.8	2.0[b]	0.9	0.8	1.3	0.9	1.6	1.3	1.0	1.4	0.9	1.2
MePyr-C1	0.9	1.4	0.9	0.8	1.6*	0.9	2.9*	1.2*	1.2	1.7*	1.1	1.4[d]
MePyr-C2	0.9	1.2	1.1	0.9	2.0*	1.1	3.0*	1.9[c]	1.4*	2.0*	1.2	1.5

Results are mentioned as control-relative gene induction (>1) or repression (<1) factors. The * sign indicates a significant difference in comparison to the control, according to *t* test for independent samples ($p<0.05$; $df=4$): [a] $p=0.069$; [b] $p=0.076$; [c] $p=0.054$; [d] $p=0.078$

observations, Fairbairn et al. (2012) reported that the exposure of *D. rerio* embryos to phenanthrene and fluorene induced morphological abnormalities resulting from the disruption of embryonic axis determination and a concomitant increase in the levels of nuclear β-catenin throughout the embryo (suggesting the aberrant activation of Wnt/β-catenin pathway). Similar observations were made in sea urchin (*Lytechinus anemesis*) embryos exposed to creosote and PAHs (Pillai et al. 2003). According to these studies, it seems that PAHs disrupt dorsal–ventral axis determination in the embryos via the Wnt/β-catenin signaling pathway (Fairbairn et al. 2012). It is thus possible that some of the spinal deformities observed in the present study following exposure of medaka embryos to Pyr and MePyr could result from Wnt signaling disturbance during somitogenesis as suggested for Cd (Chow and Cheng 2003).

Similarly, exposure of *S. marmoratus* embryos to benzo[*a*] pyrene resulted in spinal and craniofacial deformities (including lower jaw deformities) in association to the inhibition of *shh* transcription levels (He et al. 2011). Likewise, exposure of *D. rerio* embryos to TCDD caused lower jaw deformities and the *ahr2*-dependent downregulation of *shh* genes transcription (Teraoka et al. 2006). The authors of these studies concluded that craniofacial deformities induced by benzo[*a*]pyrene and TCDD could be the result of Shh signaling pathway impairment, leading to a failure of cell proliferation (He et al. 2011; Teraoka et al. 2006). Considering the antagonist interactions existing between Wnt and Shh pathways, it is possible that some spinal and craniofacial deformities observed in the present study following exposure of medaka embryos to Pyr and MePyr are the result of Wnt signaling pathway disruption, as suggested by the significant increase of *wnt1* transcription level (Table 6). Moreover, recent genomic analysis performed in a zebrafish tissue regeneration model revealed functional cross talk between AhR and the Wnt/β-catenin signal transduction pathway (Lijoy et al. 2009). It thus can be hypothesized that the AhR pathway is involved in Wnt signaling disruption as Shh pathway deregulation was shown to be AhR dependent following TCDD exposure (Teraoka et al. 2006).

Impact of Pyr and MePyr exposure on retinoid metabolism gene transcription

The impact of Pyr and MePyr exposure on retinoid metabolism was investigated through the analysis of retinoic acid receptors (*rarα1*, *rarγ1*, and *rxrα1*) and *raldh2* transcription levels. In 7 dpf embryos exposed to Pyr-C2 treatment, *rxrα1* transcription level tended to increase in comparison to the control treatment ($p=0.07$, Table 6). Similarly, exposure to MePyr-C2 concentration significantly stimulated *rarα1* transcription in medaka embryos ($p<0.05$, according to *t* test when compared to the control). These modulations of retinoic acid receptor transcripts were simultaneous to *cyp1a* transcription induction ($p<0.05$, Table 6). The *rarα1* transcription levels were still overexpressed when compared to the control in larvae exposed to both MePyr treatments ($p<0.02$) and *rxrα1* transcript level in larvae was close to significant threshold ($p=0.08$) when compared to the control in MePyr-C1 treatment. Moreover, *raldh2* gene transcripts were also significantly upregulated in newly hatched larvae exposed to the highest concentration of MePyr. It also reflected that at the protein level, the modulations of these genes could indicate an increased transformation of retinoid reserves or retinol into retinoic acid and the activation of the RXR/RAR pathway. It is

consistent with the reduction of retinoid stores correlated to CYP1A or EROD induction observed in fish exposed to PAHs (Arcand-Hoy and Metcalfe 1999; Besselink et al. 1998). Furthermore, a concentration-dependent increase of all-*trans*-retinoic acids concentration as well as CYP1A1 activity and *cyp1a1* mRNA level was observed in TCDD-exposed rats, suggesting that the CYP1A pathway is involved in retinoic acid synthesis induced by dioxin (Schmidt et al. 2003). All these observations suggest that, as for TCDD, the AhR/CYP1A pathway is involved in retinoid metabolism deregulation induced by Pyr and MePyr. Molecular and physiological interactions between retinoid signaling and AhR pathways have been investigated in medaka embryos (Hayashida et al. 2004). The study demonstrated that both retinoic acid and its receptors RXR/RAR were required for AhR mRNA expression. In particular, the study evidenced that (1) retinoic acid excess and activation of RXR/RAR receptors led to *ahr* transcription upregulation and (2) retinoic acid excess and AhR activation resulted in vascular damage and body axis malformations. Consequently, it is possible that retinoid metabolism and signaling pathway deregulation following Pyr and MePyr exposure are involved in the appearance of at least a part of skeletal and cardiovascular deformities in exposed fish ELS. However, other investigations are needed to demonstrate if retinoid system disruption plays a critical role in Pyr and MePyr teratogenicity.

Pyr and MePyr exposure modulates transcription of genes involved in mitochondrial metabolism

Gene transcription analysis performed on embryos exposed to Pyr-C2 and both MePyr treatments revealed a significant induction of *coxI* (cytochrome C oxidase subunit I) gene transcription ($p<0.05$, Table 6). *CoxI* gene product is a mitochondria-encoded subunit of complex IV of the mitochondrial respiratory chain. A significant increase of *coxI* transcript level has been already reported in the kidney and the liver of *Oncorhynchus mykiss* juveniles exposed to Pyr (Krasnov et al. 2005). The stimulation of its transcription could be interpreted as a compensatory response of embryos against exposure to Pyr and MePyr. Indeed, as COX is considered as the rate-limiting step for mitochondrial respiration, *coxI* transcript overexpression could indicate an attempt of the organism to restore a decrease in mitochondrial activity (i.e., ATP synthesis) and to efficiently consume O_2, thus limiting ROS overproduction (Achard-Joris et al. 2006). Considering that biologically activated PAHs could disrupt oxidative phosphorylation which may interrupt the mitochondrial electron transport chain, a reduction in available ATP and subsequent energy reserves has been proposed as a possible mechanism to explain the decreased hatching success in medaka ELS exposed to PAH and alkyl-PAH (Rhodes et al. 2005). A depletion of available energy stores during embryonic development could thus also be responsible for the decrease of larval growth (in Pyr- and MePyr-C2 treatments) as well as the reduced and delayed hatching events (in MePyr-C1 treatment) observed in the present study. However, it remains unclear if the impact of these PAHs on the energy reserves is the result of an impairment of the mitochondrial electron transport chain functioning and/or of an important allocation of available energy to biotransformation of xenobiotics. This latter hypothesis seems to be supported by the concomitant overexpression of *cyp1a* and *coxI* gene transcripts in medaka embryos exposed to the highest concentration of Pyr and MePyr (Table 6).

Induction of DNA damage by Pyr and MePyr

The potential induction of DNA damage by Pyr and MePyr was evaluated in 2 dph larvae using the comet assay. DNA strand breaks were not significantly induced in comparison to the control ($p>0.05$), although a concentration-dependent increase trend of the percentage of tail DNA was observed (Fig. 4). Conversely, the percentage of hedgehog cells (i.e., those with heavily DNA damaged nuclei) significantly increased in larvae from Pyr-C1 and MePyr-C2 treatments when compared to the control ($p<0.01$, Fig. 4). Moreover, *p53* transcripts were significantly overexpressed in larvae exposed to the two concentrations of MePyr ($p<0.05$, Table 6). If reflected at the protein level, *p53* induction could result in cell cycle arrest before the S phase to allow repair of DNA damage prior to DNA replication or the induction of apoptosis in cases where DNA damage is too severe to be properly repaired (Basu and Haldar 1998). DNA damage could be the result of ROS overproduction as suggested by *coxI* transcription induction (see "Pyr and MePyr exposure modulates transcription of

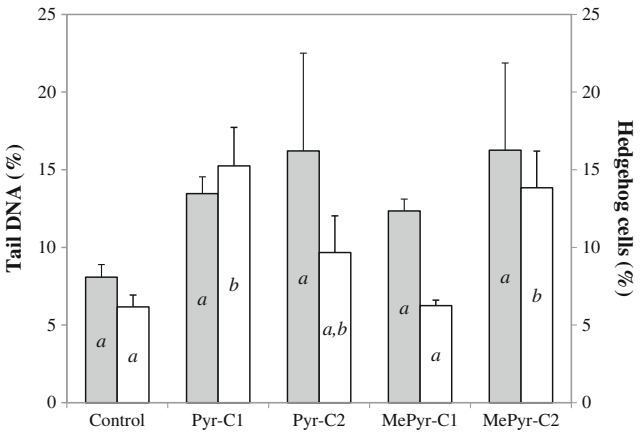

Fig. 4 DNA damage in 2 dph larvae following exposure of medaka embryos to Pyr- or MePyr-spiked sediments assessed with the comet assay. Values represent the mean response (±SD) from three replicates for the percentage of tail DNA (*gray bars*) and of hedgehog cells (*white bars*). *Different letters* indicate significant differences between treatments using one-way ANOVA followed by Tukey's post hoc test ($p<0.05$; $df=4$)

genes involved in mitochondrial metabolism"). This hypothesis is supported by *ogg1* gene expression whose encoded protein is involved in the base excision repair mechanism in the case of oxidative lesions of DNA. Indeed, *ogg1* transcripts were significantly upregulated in larvae following exposure to MePyr-C1 treatments ($p<0.05$) and close to the significant threshold ($p=0.05$ in comparison to the control; Table 6) in medaka larvae exposed to MePyr-C2 concentrations. However, no significant induction of the antioxidant *sod*(*Mn*) and *sod*(*Cu*/*Zn*) gene transcripts was noticeable to confirm ROS overproduction following exposure to Pyr and MePyr ($p>0.05$ in comparison to the control; Table 6).

In summary, the present study demonstrated (1) no significant induction of DNA strand breaks (illustrated by the percentage of tail DNA) by either Pyr or MePyr; (2) a significant increase in the percentage of hedgehog cells by Pyr and MePyr; and (3) induction of *p53* and *ogg1* transcription levels following MePyr exposure. Further investigations are needed to conclude on the impact of Pyr exposure on DNA integrity in medaka ELS. However, we could hypothesize that MePyr exposure induces oxidative DNA damage that is fully repaired by DNA repair enzymes (such as Ogg1), except in the case of heavily DNA-damaged cells (i.e., hedgehog cells) in which apoptosis could be initiated through the *p53* pathway. This latter hypothesis is supported by the observation of cell death in the brain and the spinal cord of *D. rerio* embryos exposed to Pyr (Incardona et al. 2004). Apoptotic cell death was also reported in medaka embryonic vasculature following TCDD exposure (Cantrell et al. 1998).

Interestingly, *p53* transcription overexpression following MePyr exposure was simultaneous to *wnt1* transcription level induction (Table 6). There is little evidence to suggest that an abnormal activation of the Wnt pathway (including the *wnt1* gene) could deregulate the normal ontogenesis process by affecting cell differentiation (L'Allemain 2006). Moreover, aberrant Wnt signaling has been reported to be involved in some development of cancers which most likely results from inappropriate gene activation mediated by stabilized β-catenin (Polakis 2000; L'Allemain 2006). Recently, an antidifferentiation function of p53 through direct regulation of the Wnt signaling pathway was highlighted in mouse embryonic stem cells (Lee et al. 2010). The authors concluded that p53 could become "tumorigenic" if the induction of Wnt ligands by p53 is inherited aberrantly by the progeny cells of embryonic stem cells. Further specific studies on the implication of p53 and Wnt pathways in ontogenesis mechanisms of fish embryos could bring new insights into the potential carcinogenicity of MePyr.

Implication of CYP1A pathway in Pyr and MePyr toxicity

The overall toxic effects of Pyr and MePyr in medaka ELS highlighted in the present study overlapped considerably with those induced following TCDD exposure. Such similarities between Pyr and TCDD toxicity have been already reported and suggest the involvement of the AhR/CYP1A metabolism pathway (e.g., Hendon et al. 2008; Incardona et al. 2005, 2006).

Supporting this hypothesis, *cyp1A* transcription levels were significantly induced when compared to the control in embryos exposed to the highest concentration of Pyr and MePyr ($p<0.05$, Table 6). *Cyp1a* induction factors were moderate with values equal to 1.8 and 2.5 for Pyr and MePyr, respectively, which seem to be in agreement with their relative AhR agonist potency in comparison with other strong AhR agonists such as TCDD or benzo[*a*]pyrene (Barron et al. 2004). *Cyp1a* transcript induction was still noticeable in larvae from the Pyr-C2 treatment with a *p* value close to the significant threshold in comparison to the control ($p=0.076$).

CYP1A induction was reported throughout the vascular endothelium and the liver of *D. rerio* larvae exposed to Pyr (Incardona et al. 2006). The induction of this enzyme preceded and accompanied the emergence of developmental defects (including dorsal curvature, anemia, edemas, cell death, and reduced peripheral circulation) and systemic toxicity induced by Pyr exposure. Moreover, Pyr-induced mortality was time coincident with alterations in the appearance of the liver (Incardona et al. 2006). Gene silencing with *ahr2* antisense morpholino largely prevented teratogenicity and lethal effects of Pyr in *D. rerio* embryos and also markedly reduced the levels of CYP1A induction (Incardona et al. 2005). Similarly, an *ahr1a* morpholino injection partially improved the resistance of embryos to Pyr toxicity, including normal liver appearance and absence of pericardial edemas and neural tube cell death. *Cyp1a* knockdown also reduced defects in embryos exposed to Pyr (Incardona et al. 2005). Moreover, Pyr-induced lethality was prevented or markedly delayed by several hours in *cyp1a*, *ahr1*, and *ahr2* morphants (Incardona et al. 2005, 2006). Evidence gathered in these studies indicates that (1) the toxic effects of Pyr are clearly AhR/CYP1A dependent; (2) the metabolism of Pyr by CYP1A in the vascular endothelium probably contributes to the emergence of some teratogenic effects, in particular dorsal curvature; and (3) hepatic CYP1A activity strongly contributes to the systemic toxicity of Pyr, probably through the formation of Pyr toxic metabolite(s) (Incardona et al. 2005, 2006).

This last assumption is supported by the positive correlation between DNA damage and the level of biliary hydroxylated metabolites (mainly 1-OH-Pyr) observed in juvenile flatfish (*Solea solea*) exposed to a mixture of benzo[*a*]pyrene, fluoranthene, and pyrene (Wessel et al. 2010). The authors concluded that PAH-induced DNA strand breaks probably result from the induction of oxidative stress by prooxidant PAH metabolites and the excision activity of DNA repair enzymes. Furthermore, it has been demonstrated that ROS formation could occur during the CYP1A catalytic cycle or in

a latter step of PAH biotransformation, during quinones redox cycle (Baulig et al. 2003; Morel et al. 1999). To conclude, it seems that the AhR/CYP1A pathway is strongly involved in Pyr and MePyr toxic effects as it could contribute, directly or indirectly, to ROS overproduction, genotoxicity, teratogenicity and, finally, systemic toxicity of both compounds.

Conclusion

The effects of environmental concentrations of Pyr and MePyr were investigated in medaka ELS exposed by sediment contact. Both compounds strongly impacted medaka embryonic development, with the cardiovascular system as primary target of toxicity. Developmental abnormalities also included spinal and jaw deformities observed in medaka larvae following Pyr and MePyr exposure considerably overlapped those induced by TCDD. In addition, the transcription level of several genes involved in mitochondrial metabolism, cell differentiation and proliferation control, cell cycle arrest, and retinoid metabolism was significantly deregulated. A significant increase in *cyp1a* transcript levels suggested that the AhR/CYP1A pathway is involved in several toxic effects induced by Pyr and MePyr exposure. Overall, the results showed that exposure to the tested environmental concentrations of Pyr and MePyr in sediment has a clear impact on the development of medaka embryos resulting in noticeable effects at both phenotypical and transcriptional levels. These observations highlight the ecotoxicological risk presented by these compounds in PAH-impacted areas. The present study also showed new aspects of the mode of action of Pyr, and for the first time, the effects of MePyr were investigated in fish ELS. With regards to the efficiency of the MELAc and the relevance of the route of exposure, this approach could be applied to the investigation of the toxico-kinetics and toxico-dynamics of various chemicals including particle-bound pollutants in fish ELS.

Acknowledgments This study was supported by the Aquitaine Region, the Seine-Aval Program, the French National Program EC2CO (GenerationPop Research Project), and the University of Bordeaux 1. Iris Barjhoux received a PhD fellowship from the Ministère de l'Enseignement Supérieur et de la Recherche (France).

References

Achard-Joris M, Gonzalez P, Marie V, Baudrimont M, Bourdineaud JP (2006) Cytochrome *c* oxydase subunit I gene is up-regulated by cadmium in freshwater and marine bivalves. BioMetals 19:237–244

Antkiewicz DS, Burns CG, Carney SA, Peterson RE, Heideman W (2005) Heart malformation is an early response to TCDD in embryonic zebrafish. Toxicol Sci 84:368–377

Arcand-Hoy LD, Metcalfe CD (1999) Biomarkers of exposure of brown bullheads (*Ameiurus nebulosus*) to contaminants in the lower Great Lakes, North America. Environ Toxicol Chem 18:740–749

Barjhoux I, Baudrimont M, Morin B, Landi L, Gonzalez P, Cachot J (2012) Effects of copper and cadmium spiked-sediments on embryonic development of Japanese medaka (*Oryzias latipes*). Ecotoxicol Environ Saf 79:272–282

Barron MG, Heintz R, Rice SD (2004) Relative potency of PAHs and heterocycles as aryl hydrocarbon receptor agonists in fish. Mar Environ Res 58:95–100

Basu A, Haldar S (1998) The relationship between Bcl2, Bax and p53: consequences for cell cycle progression and cell death. Mol Human Reprod 4:1099–1109

Baulig A, Garlatti M, Bonvallot V, Marchand A, Barouki R, Marano F, Baeza-Squiban A (2003) Involvement of reactive oxygen species in the metabolic pathways triggered by diesel exhaust particles in human airway epithelial cells. Am J Physiol Lung Cell Mol Physiol 285:L671–L679

Besselink HT, Flipsen E, Eggens ML, Vethaak AD, Koeman JH, Brouwer A (1998) Alterations in plasma and hepatic retinoid levels in flounder (*Platichthys flesus*) after chronic exposure to contaminated harbour sludge in a mesocosm study. Aquat Toxicol 42:271–285

Billiard SM, Querbach K, Hodson PV (1999) Toxicity of retene to early life stages of two freshwater fish species. Environ Toxicol Chem 18: 2070–2077

Billiard SM, Meyer JN, Wassenberg DM, Hodson PV, Di Giulio RT (2008) Nonadditive effects of PAHs on early vertebrate development: mechanisms and implications for risk assessment. Toxicol Sci 105:5–23

Boily M, Bisson M, Spear PA (2004) Retinoids—biomarkers and molecular basis for chemicals toxic effects (Rétinoïdes - Biomarqueurs et base moléculaire d'effets de substances toxiques). In: Pelletier E, Campbell PGC, Denizeau F (eds) Ecotoxicologie Moléculaire—Principes fondamentaux et perspectives de développement. Presses de l'Université du Québec, Sainte-Foy, Québec, pp 197–256

Brinkworth LC, Hodson PV, Tabash S, Lee P (2003) CYP1A induction and blue sac disease in early developmental stages of rainbow trout (*Oncorhynchus mykiss*) exposed to retene. J Toxicol Environ Health A 66:627–646

Cachot J, Geffard O, Augagneur S, Lacroix S, Le Menach K, Peluhet L, Couteau J, Denier X, Devier MH, Pottier D, Budzinski H (2006) Evidence of genotoxicity related to high PAH content of sediments in the upper part of the Seine estuary (Normandy, France). Aquat Toxicol 79:257–267

Cachot J, Law M, Pottier D, Peluhet L, Norris M, Budzinski H, Winn R (2007) Characterization of toxic effects of sediment-associated organic pollutants using the lambda transgenic medaka. Environ Sci Technol 41:7830–7836

Cantrell SM, Joy-Schlezinger J, Stegeman JJ, Tillitt DE, Hannink M (1998) Correlation of 2,3,7,8-tetrachlorodibenzo-*p*-dioxin-induced apoptotic cell death in the embryonic vasculature with embryotoxicity. Toxicol Appl Pharm 148:24–34

Carls MG, Rice SD, Hose JE (1999) Sensitivity of fish embryos to weathered crude oil: part I. Low-level exposure during incubation causes malformations, genetic damage, and mortality in larval pacific herring (*Clupea pallasi*). Environ Toxicol Chem 18:481–493

Carls MG, Holland L, Larsen M, Collier TK, Scholz NL, Incardona JP (2008) Fish embryos are damaged by dissolved PAHs, not oil particles. Aquat Toxicol 88:121–127

Chow ESH, Cheng SH (2003) Cadmium affects muscle type development and axon growth in zebrafish embryonic somitogenesis. Toxicol Sci 73:149–159

de Perre C, Le Ménach K, Ibalot F, Parlanti E, Budzinski H (2014) Development of solid-phase microextraction to study dissolved organic matter—polycyclic aromatic hydrocarbon interactions in aquatic environment. Anal Chim Acta 807:51–60

Denison MS, Heath-Pagliuso S (1998) The Ah receptor: a regulator of the biochemical and toxicological actions of structurally diverse chemicals. Bull Environ Contam Toxicol 61:557–568

Devier M-H, Augagneur S, Budzinski H, Le Menach K, Mora P, Narbonne J-F, Garrigues P (2005) One-year monitoring survey of organic compounds (PAHs, PCBs, TBT), heavy metals and biomarkers in blue mussels from the Arcachon Bay, France. J Environ Monit 7:224–240

Dupree C, Ahrens A (2007) Polycyclic aromatic hydrocarbons in Auckland's aquatic environment: source concentrations and potential environmental risks. Prepared by NIWA for Auckland Regional Council Auckland Regional Council Technical Publication No 378

Elonen GE, Spehar RL, Holcombe GW, Johnson RD, Fernandez JD, Erickson RJ, Tietge JE, Cook PM (1998) Comparative toxicity of 2, 3,7,8-tetrachlorodibenzo-*p*-dioxin to seven freshwater fish species during early life-stage development. Environ Toxicol Chem 17: 472–483

Fairbairn EA, Bonthius J, Cherr GN (2012) Polycyclic aromatic hydrocarbons and dibutyl phthalate disrupt dorsal–ventral axis determination via the *Wnt*/β-*catenin* signaling pathway in zebrafish embryos. Aquat Toxicol 124–125:188–196

Farwell A, Nero V, Croft M, Bal P, Dixon DG (2006) Modified Japanese medaka embryo-larval bioassay for rapid determination of developmental abnormalities. Arch Environ Contam Toxicol 51:600–607

Feng S, Cao Z, Wang X (2013) Role of aryl hydrocarbon receptor in cancer. Biochim Biophys Acta 1836:197–210

Geffard O, Geffard A, His E, Budzinski H (2003) Assessment of the bioavailability and toxicity of sediment-associated polycyclic aromatic hydrocarbons and heavy metals applied to *Crassostrea gigas* embryos and larvae. Mar Pollut Bull 46:481–490

Glatt H, Rost K, Frank H, Seidel A, Kollock R (2008) Detoxification of promutagenic aldehydes derived from methylpyrenes by human aldehyde dehydrogenases ALDH2 and ALDH3A1. Arch Biochem Biophys 477:196–205

Hartmann A, Agurell E, Beevers C, Brendler-Schwaab S, Burlinson B, Clay P, Collins A, Smith A, Speit G, Thybaud V, Tice RR (2003) Recommendations for conducting the *in vivo* alkaline Comet assay. Mutagenesis 18:45–51

Hayashida Y, Kawamura T, Hori-e R, Yamashita I (2004) Retinoic acid and its receptors are required for expression of aryl hydrocarbon receptor mRNA and embryonic development of blood vessel and bone in the medaka fish, *Oryzias latipes*. Zool Sci 21:541–551

He C, Zuo Z, Shi X, Li R, Chen D, Huang X, Chen Y, Wang C (2011) Effects of benzo(a)pyrene on the skeletal development of *Sebastiscus marmoratus* embryos and the molecular mechanism involved. Aquat Toxicol 101:335–341

Heister K, Pols S, Gustav Loch JP, Bosma TNP (2013) Desorption behaviour of polycyclic aromatic hydrocarbons after long-term storage of two harbour sludges from the port of Rotterdam, The Netherlands. J Soils Sed 13:1113–1122

Hendon LA, Carlson EA, Manning S, Brouwer M (2008) Molecular and developmental effects of exposure to pyrene in the early life-stages of *Cyprinodon variegates*. Comp Biochem Physiol C - Toxicol Pharmacol 147:205–215

Hollert H, Keiter S, König N, Rudolf M, Ulrich M, Braunbeck T (2003) A new sediment contact assay to assess particle-bound pollutants using zebrafish (*Danio rerio*) embryos. J Soils Sed 3:197–207

Honkanen JO, Wiegand C, Kukkonen JVK (2008) Humic substances modify accumulation but not biotransformation of pyrene in salmon yolk-sac fry. Aquat Toxicol 86:239–248

Hornung MW, Spitsbergen JM, Peterson RE (1999) 2,3,7,8-tetrachlorodibenzo-p-dioxin alters cardiovascular and craniofacial development and function in sac fry of rainbow trout (*Oncorhynchus mykiss*). Toxico Sci 47:40–51

Hornung MW, Cook PM, Fitzsimmons PN, Kuehl DW, Nichols JW (2007) Tissue distribution and metabolism of benzo[a]pyrene in embryonic and larval medaka (*Oryzias latipes*). Toxicol Sci 100: 393–405

Incardona JP, Collier TK, Scholz NL (2004) Defects in cardiac function precede morphological abnormalities in fish embryos exposed to polycyclic aromatic hydrocarbons. Toxicol Appl Pharmacol 196: 191–205

Incardona JP, Carls MG, Teraoka H, Sloan CA, Collier TK, Scholz NL (2005) Aryl hydrocarbon receptor-independent toxicity of weathered crude oil during fish development. Environ Health Perspect 113:1755–1762

Incardona JP, Day HL, Collier TK, Scholz NL (2006) Developmental toxicity of 4-ring polycyclic aromatic hydrocarbons in zebrafish is differentially dependent on AH receptor isoforms and hepatic cytochrome P4501A metabolism. Toxicol Appl Pharmacol 217:308–321

Ineris (2006) PAHs—techno-economic data on chemical substances in France (HAP - Données technico-économiques sur les substances chimiques en France). Last update: April 2006, pp 1-45

Kimbrough KL, Dickhut RM (2006) Assessment of polycyclic aromatic hydrocarbon input to urban wetlands in relation to adjacent land use. Mar Pollut Bull 52:1355–1363

Kocan RM, Matta MB, Salazar SM (1996) Toxicity of weathered coal tar for shortnose sturgeon (*Acipenser brevirostrum*) embryos and larvae. Arch Environ Contam Toxicol 31:161–165

Krasnov A, Koskinen H, Rexroad C, Afanasyev S, Molsa H, Oikari A (2005) Transcriptome responses to carbon tetrachloride and pyrene in the kidney and liver of juvenile rainbow trout (*Oncorhynchus mykiss*). Aquat Toxicol 74:70–81

Kumaravel TS, Vilhar B, Faux SP, Jha AN (2009) Comet assay measurements: a perspective. Cell Biol Toxicol 25:53–64

L'Allemain G (2006) Role of the Wnt pathway in oncogenesis (Rôle des voies Wnt dans l'oncogénèse). Bull Cancer 93:88–97

Lee K-H, Li M, Michalowski AM, Zhang X, Liao H, Chen L, Xu Y, Wu X, Huang J (2010) A genomewide study identifies the Wnt signaling pathway as a major target of p53 in murine embryonic stem cells. Proc Natl Acad Sci U S A 107(1):69–74

Letellier M, Budzinski H, Bellocq J, Connan J (1999) Focused microwave-assisted extraction of polycyclic aromatic hydrocarbons and alkanes from sediments and source rocks. Org Geochem 30: 1353–1365

Li R, Zuo Z, Chen D, He C, Chen R, Chen Y, Wang C (2011) Inhibition by polycyclic aromatic hydrocarbons of ATPase activities in *Sebastiscus marmoratus* larvae: relationship with the development of early life stages. Mar Environ Res 71:86–90

Liehr GA, Heise S, Ahlf W, Offermann K, Witt G (2013) Assessing the risk of a 50-year-old dump site in the Baltic Sea by combining chemical analysis, bioaccumulation, and ecotoxicity. J Soils Sed 13:1270–1283

Lijoy MK, Simonich MT, Tanguay RL (2009) AHR-dependent misregulation of Wnt signaling disrupts tissue regeneration. Biochem Pharmacol 77(4):498–507

Livak KJ, Schmittgen TD (2001) Analysis of relative gene expression data using real-time quantitative PCR and the $2^{-\Delta CT}$ method. Methods 25:402–408

Long ER, Macdonald DD, Smith SL, Calder FD (1995) Incidence of adverse biological effects within ranges of chemical concentrations in marine and estuarine sediments. Environ Manage 19:81–97

MacDonald DD, Carr RS, Calder FD, Long ER, Ingersoll CG (1996) Development and evaluation of sediment quality guidelines for Florida coastal waters. Ecotoxicology 5:253–278

MacDonald DD, Ingersoll CG, Berger TA (2000) Development and evaluation of consensus-based sediment quality guidelines for freshwater ecosystems. Arch Environ Contam Toxicol 39:20–31

Mhadhbi L, Boumaiza M, Beiras R (2010) A standard ecotoxicological bioassay using early life stages of the marine fish *Psetta maxima*. Aquat Living Resour 23:209–216

Monien BH, Müller C, Engst W, Frank H, Seidel A, Glatt H (2008) Time course of hepatic 1-methylpyrene DNA adducts in rats determined

by isotope dilution LC-MS/MS and ^{32}P-postlabeling. Chem Res Toxicol 21:2017–2025

Morel Y, Mermod N, Barouki R (1999) An autoregulatory loop controlling CYP1A1 gene expression: role of H_2O_2 and NFI. Mol Cell Biol 19:6825–6832

Morin B, Filatreau J, Vicquelin L, Barjhoux I, Guinel S, Leray-Forget J, Cachot J (2011) Detection of DNA damage in yolk-sac larvae of the Japanese Medaka, *Oryzias latipes*, by the comet assay. Anal Bioanal Chem 399:2235–2242

Münsterberg AE, Kitajewski J, Bumcrot DA, McMahon AP, Lassar AB (1995) Combinatorial signaling by Sonic hedgehog and Wnt family members induces myogenic bHLH gene expression in the somite. Genes Dev 9:2911–2922

Nagy AS, Simon G, Szabo J, Vass I (2013) Polycyclic aromatic hydrocarbons in surface water and bed sediments of the Hungarian upper section of the Danube River. Environ Monit Assess 185:4619–4631

Notar M, Leskovsek H, Faganeli J (2001) Composition, distribution and sources of polycyclic aromatic hydrocarbons in sediments of the Gulf of Trieste, northern Adriatic Sea. Mar Pollut Bull 42:36–44

Novak J, Benisek M, Hilscherova K (2008) Disruption of retinoid transport, metabolism and signaling by environmental pollutants. Environ Int 34:898–913

Olive PL, Banath JP (1995) Sizing highly fragmented DNA in individual apoptotic cells using the comet assay and a DNA crosslink. Agent Exp Cell Res 221:19–26

Pancirov RJ, Brown RA (1977) Polynuclear aromatic hydrocarbons in marine tissues. Environ Sci Technol 11:989–992

Petersen GI, Kristensen P (1998) Bioaccumulation of lipophilic substances in fish early life stages. Environ Toxicol Chem 17:1385–1395

Pillai MC, Vines CA, Wikramanayake AH, Cherr GN (2003) Polycyclic aromatic hydrocarbons disrupt axial development in sea urchin embryos through a β-catenin dependent pathway. Toxicology 186:93–108

Polakis P (2000) Wnt signaling and cancer. Genes Dev 14:1837–1851

Rhodes S, Farwell A, Hewitt LM, MacKinnon M, Dixon DG (2005) The effects of dimethylated and alkylated polycyclic aromatic hydrocarbons on the embryonic development of the Japanese medaka. Ecotoxicol Environ Saf 60:247–258

Rolland RM (2000) A review of chemically-induced alterations in thyroid and vitamin A status from field studies of wildlife and fish. J Wild Dis 36:615–635

Sanchez-Avila J, Vicente J, Echavarri-Erasun B, Porte C, Tauler R, Lacorte S (2013) Sources, fluxes and risk of organic micropollutants to the Cantabrian Sea (Spain). Mar Pollut Bull 72:119–132

Schmidt CK, Hoegberg P, Fletcher N, Nilsson CB, Trossvik C, Hakansson H, Nau H (2003) 2,3,7,8-Tetrachlorodibenzo-*p*-dioxin (TCDD) alters the endogenous metabolism of all-*trans*-retinoic acid in the rat. Arch Toxicol 77:371–383

Shimada T (2006) Xenobiotic-metabolizing enzymes involved in activation and detoxification of carcinogenic polycyclic aromatic hydrocarbons. Drug Metab Pharmacokinet 21:257–276

Sverdrup LE, Nielsen T, Krogh PH (2002) Soil ecotoxicity of polycyclic aromatic hydrocarbons in relation to soil sorption, lipophilicity, and water solubility. Environ Sci Technol 36:2429–2435

Teraoka H, Dong W, Ogawa S, Tsukiyama S, Okuhara Y, Niiyama M, Ueno N, Peterson RE, Hiraga T (2002) 2,3,7,8-Tetrachlorodibenzo-*p*-dioxin toxicity in the zebrafish embryo: altered regional blood flow and impaired lower jaw development. Toxicol Sci 65:192–199

Teraoka H, Dong W, Okuhara Y, Lwasa H, Shindo A, Hill AJ, Kawakami A, Hiraga T (2006) Impairment of lower jaw growth in developing zebrafish exposed to 2,3,7,8-tetrachlorodibenzo-*p*-dioxin and reduced hedgehog expression. Aquat Toxicol 78:103–113

Turcotte D, Akhtar P, Bowerman M, Kiparissis Y, Brown RS, Hodson PV (2011) Measuring the toxicity of alkyl-phenanthrenes to early life stages of medaka (*Oryzias latipes*) using partition-controlled delivery. Environ Toxicol Chem 30:487–495

Ulloa F, Marti E (2010) Wnt won the war: antagonistic role of Wnt over Shh controls dorso-ventral patterning of the vertebrate neural tube. Dev Dynam 239:69–76

Vicquelin L, Leray-Forget J, Peluhet L, LeMenach K, Deflandre B, Anschutz P, Etcheber H, Morin B, Budzinski H, Cachot J (2011) A new spiked sediment assay using embryos of the Japanese medaka specifically designed for a reliable toxicity assessment of hydrophobic chemicals. Aquat Toxicol 105:235–245

Wang X-C, Zhang Y-X, Chen RF (2001) Distribution and partitioning of polycyclic aromatic hydrocarbons (PAHs) in different size fractions in sediments from Boston harbor, United States. Mar Pollut Bull 42:1139–1149

Wessel N, Santos R, Menard D, Le Menach K, Buchet V, Lebayon N, Loizeau V, Burgeot T, Budzinski H, Akcha F (2010) Relationship between PAH biotransformation as measured by biliary metabolites and EROD activity, and genotoxicity in juveniles of sole (*Solea solea*). Mar Environ Res 69:S71–S73